



<b>Experiment title:</b> Temperature dependence of the electric field-induced phase transformation in the promising lead-free Ba(Zr <sub>0.2</sub> Ti <sub>0.8</sub> ) O <sub>3</sub> -(Ba <sub>0.7</sub> Ca <sub>0.3</sub> ) TiO <sub>3</sub> ferroelectric materials.	<b>Experiment number:</b> A25-2-1039	
<b>Beamline:</b> BM25 Spline	<b>Date of experiment:</b> from: 26 Jan 2023 at 8:00 to: 30 Jan 2023 at 8:00	<b>Date of report:</b> 27 April 2023  <i>Received at ESRF:</i>
<b>Shifts:</b> 12	<b>Local contact(s):</b> Dr. Juan RUBIO ZUAZO	
<b>Names and affiliations of applicants</b> (* indicates experimentalists):  *Diego A. Ochoa, José E. García and Samuel López Blanco Universitat Politècnica de Catalunya / Barcelona / Spain  *Harvey Amorín Instituto de Ciencia de Materiales de Madrid (ICMM), CSIC / Madrid / Spain		

## Report:

### Summary

Experiments focused on investigating the outstanding properties of Ba(Zr<sub>0.2</sub>Ti<sub>0.8</sub>) O<sub>3</sub>-(Ba<sub>0.7</sub>Ca<sub>0.3</sub>) TiO<sub>3</sub> from now on BCZT. The experiments investigate the controversial origin of the giant strain response and the low strain hysteresis of the lead-free BZCT piezoceramic system with tailored microstructure. High-resolution XRD measurements on poled and unpoled samples with different grain sizes were performed at different temperatures to gain insights into two different phenomena existing in this material. The first one, the electric-field-induced phase transformation, consists of the phase boundary movement due to an externally applied electric field. Meanwhile, the second, the motion of the domain walls, refers to the movement of the domain walls and, consequently, a change in the domain configuration induced by the applied electric field. Both phenomena are related to the outstanding functional properties of BCZT, and their study becomes significant in order to elucidate the origin of these functional properties.

### Experiments description

Polycrystalline samples of BCZT composition with different grain sizes of 0.5, 5, and 30  $\mu\text{m}$  and fully dense (above 99%) microstructure were studied. Materials were cut into 10 mm  $\times$  2 mm  $\times$  1 mm samples. A thick gold layer was sputter-coated onto the 10  $\times$  1 mm<sup>2</sup> sample faces to ensure good electrical contact, while the 10  $\times$  2 mm<sup>2</sup> faces (exposed to the x-ray beam) were polished. The experiment was carried out in transmission geometry at a beam energy of 20 keV and a beam size of 0.1  $\times$  0.1 mm<sup>2</sup>.

2D diffraction patterns were collected at different applied electric fields and temperatures. The samples were introduced in a liquid nitrogen cryogenic system (Oxford OX), sweeping temperatures from 200K to 400K. This setup is optimized to facilitate the beam's alignment and guarantee that the incident X-ray beam does not interact with the gold electrodes. Two X-ray transparent Kapton tape windows, at 180 degrees from each other, were used to maintain the vacuum while allowing the X-ray beam to pass through the windows. Two different XRD measurements were performed. The room temperature XRD measurement was performed from the cryogenics system in a two-theta range from 5 to 50 degrees. Meanwhile, the XRD measurement at different temperatures, with the sample inside the cryogenic system, was limited to studying the 200, 220, 222, 400, and 440 reflections.

## Preliminary results

One of the most important preliminary results is the peak analysis of the XRD patterns for comparison between samples obtained by conventional sintering route and flash sintering.

All significant coarse-grained BCZT and CCF reflections can be indexed to a perovskite structure. Fig. 1 displays three significant reflections showing a phase combination in the coarse-grained BCZT. The 222 reflection shows an asymmetry that does not correspond to a single tetragonal phase. In addition, 400 and 440 reflections show a distribution of intensities that better correspond to a mix of phases than to a single tetragonal phase. These results lead to assume that the coarse-grained BCZT composition is in a PPB. The PPB occurs between the Orthorhombic  $Amm2$  phase and the Tetragonal  $P4mm$  phase, and it is the region at which the functional properties maximize. Meanwhile, for the CCF samples, the reflections show a pseudo-cubic phase. This pseudo-cubic phase does not explain the high field-induced strain response shown in these CCF samples, leading to thinking that other mechanisms, like electric-field-induced phase transformations, could be present.

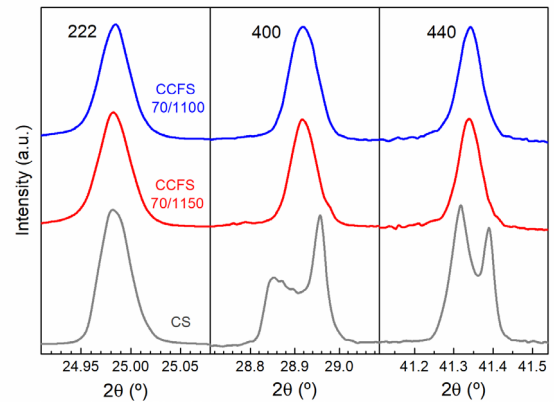


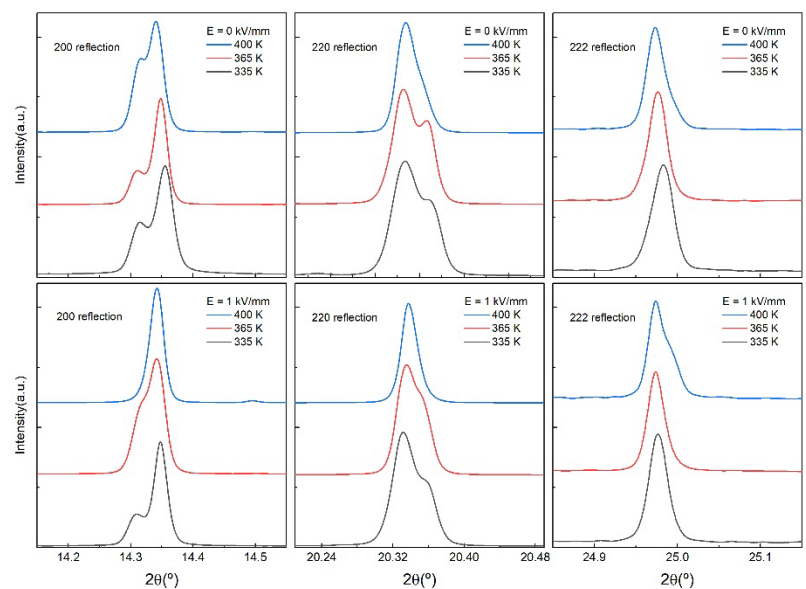
Figure 1. Comparison between two flash sintering samples (CCFS) and one conventional sintering sample (CS).

These results are part of an under-review paper recently sent to the Journal of the European Ceramic Society. Title: Fine-grained high-performance  $Ba_{0.85}Ca_{0.15}Zr_{0.1}Ti_{0.9}O_3$  piezoceramics obtained by current controlled flash sintering of nanopowders.

Figure 2 compares XRD patterns at  $E = 0$  kV/mm and  $E = 1$  kV/mm at different temperatures for representative reflections.

The preliminary results show significant variations of the XRD patterns with the applied electric field, indicating that there could be an electric-field-induced phase transformation.

The data obtained will allow us to study both the intrinsic phenomena associated with the movement of the position of the maximum of the peaks and the extrinsic phenomena associated with the movement of the domain walls. The peak analysis results will be compared with those from the room-temperature XRD patterns performed in a broader range of two thetas (not shown in this experimental report).



Finally, Figure 3 shows the results related to the study of the XRD pattern evolution in temperature for poled and unpoled samples. The phase diagram and, in consequence, crystallographic phase evolution of BCZT in temperature remains controversial. Some authors show a crystallographic phase evolution including 4 different crystallographic phases (rhombohedral to orthorhombic to tetragonal to cubic) with increased temperature from 200 to 350 K. Meanwhile, other authors include only 3 crystallographic phases (rhombohedral to tetragonal to cubic) excluding the orthorhombic phase. The measurements carried out during the beamtime focused on studying this crystallographic evolution in poled and unpoled samples.

Figure 3 clearly shows a different evolution of the crystallographic phases in temperature between the unpoled and poled samples which shows that the polarization of the samples tends to stabilize some crystallographic phases to the detriment of others.

This is a work still in progress. Nevertheless, the preliminary results show satisfactory outcomes with prospects to be published in future papers.

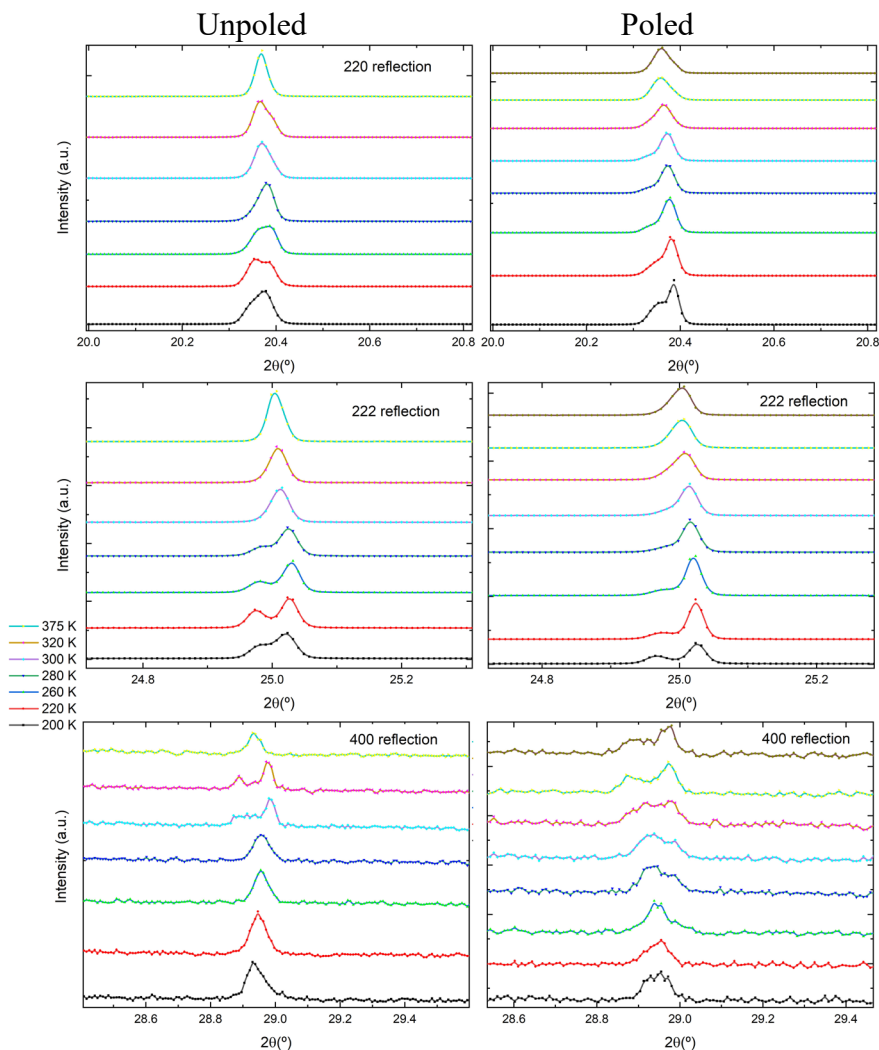


Figure 3. Evolution of the XRD patterns in temperature for poled and unpoled samples.

Once all the results referring to this beamtime have been published, the experimental report will be updated, and the corresponding references to the published articles will be sent so that they appear in the ESRF database.